2023 IMEKO TC-4 International Conference on
Metrology for Archaeology and Cultural Heritage
Rome, Italy, October 19-21, 2023

Synthesis of titania nanoparticles in W/O microemulsion: moving the production toward a green approach

Eleonora Marconi[1,3] and Luca Tortora[1,2,3]

[1] *Istituto Nazionale di Fisica Nucleare (INFN), Tre via della Vasca Navale 84, Roma, 00146, Italy*
[2] *Dipartimento di Scienze dell'università di Roma Tre, via della Vasca Navale 84, Roma, 00146, Italy*
[3] *Laboratorio Analisi Superfici Roma Tre LASR3, via della Vasca Navale 84, Roma, 00146, Italy*

***Abstract* – In this work, we report an easy, fast, reproducible, and low-temperature microemulsion procedure for the large-scale production of titania nanoparticles (NPs). The synthesis involves a polycondensation reaction of alkoxide precursors during the heating at 70 °C. A W/O microemulsion with a volume ratio of 1:1 was obtained using cetylpyridinium bromide (CPB) as a cationic surfactant. Structural and functional characterization of the samples was conducted using X-Ray Diffraction (XRD) and Scanning Electron Microscopy (SEM). The photoactivity of the nanostructured titania was evaluated by measuring the photodegradation of Methylene blue (MB). The results indicate that the photoactivity depends on the sinterization grade of the titania nanoparticles. Commercial titania nanoparticles (P25) were used as a reference material commonly employed for coating stone protection in the field of Cultural Heritage Conservation.**

I. INTRODUCTION

Architectural surfaces exposed outdoors are susceptible to soiling, including darkening caused by the accumulation of particulate matter, primarily fine carbonaceous particles rich in dark elemental carbon. In the case of carbonatic substrates (such as marble or travertine), darkening can occur through atmospheric particle deposition or the formation of "black crusts" due to a chemical reaction known as sulfation, which is triggered by the presence of atmospheric SOx [1]. While surface-deposited particles can be removed through dusting or rinsing with water, cleaning black crusts requires more advanced techniques like the use of chemicals such as EDTA (Ethylenediaminetetraacetic acid) or laser cleaning. In addition to affecting the aesthetic appearance of buildings and monuments, soiling is harmful to the conservation of carbonate stones because it promotes sulfation and thermal degradation [2]. Efforts have been made to reduce atmospheric pollutants and minimize soiling, but it remains a challenge due to oil particulates and organic carbon. A self-cleaning approach using photocatalytic surfaces is a promising solution to prevent soiling and maintain cleanliness [3]. Photocatalytic materials can oxidize contaminants and bio-organisms through redox reactions that occur on their surfaces when electron/hole pairs, generated by light irradiation, migrate to the surface. Among photocatalytic materials, TiO_2 (in the mineral forms of anatase and rutile) has been extensively studied and utilized due to its high photoactivity, stability, and cost-effectiveness among semiconductor metal oxides [4]. In newly constructed buildings, the photocatalytic activity of TiO_2 has been harnessed by incorporating nanoparticles into paints [5] mortars, tiles [6], and glasses [7] to achieve self-cleaning, antimicrobial, smog-eating, and air-purifying functionalities. TiO_2, thanks to its properties, can be employed in the field of Cultural Heritage as a "smog-eating" and self-cleaning coating [8], as well as a biocide [9], [10]. TiO_2 nanoparticles are typically dispersed in a transparent polymeric film to create an adhesive material and crack-free coatings for stone [11] to provide coating film protection for building walls. Moreover, coating with titania nanoparticles creates a self-cleaning surface thanks to the hydrophobic/hydrophilic ability after solar irradiation [12], preventing soiling and maintaining cleanliness on architectural substrates. In recent years, Degussa P25 TiO_2 nanoparticles have set the standard for photo-reactivity in environmental volatile organic compounds (VOC) applications. Degussa P25 is a non-porous 70:30% (anatase to rutile) nanoparticle, having a rutile phase but considered even more reactive than pure anatase [13].

The most common industrial process for producing titanium dioxide involves extracting TiO_2 from the ilmenite mineral. Other less common titanium oxide-bearing minerals include pseudobrookite (Fe_2TiO_5), perovskite ($CaTiO_3$), pyrophanite ($MnTiO_3$), and geikielite [(Mg, Fe)TiO_3]. Ilmenite (FeTiO3) accounts for nearly 92% of the world's consumption of titanium minerals, and almost 95% of the titanium minerals are used to produce TiO_2 pigment products [14], [15].

Various strategies have been explored to minimize the environmental impact of titania nanoparticle production, including chemical, physical, and biological synthesis

methods [16], [17]. Among the chemical synthesis methods, sol-gel, hydrothermal, and microemulsion techniques are the most commonly employed [18], [19]. The synthesis of titania nanoparticles is influenced by several factors, including the choice of precursor (alkoxide or metal salt), calcination temperature, and the type of surfactant (ionic, non-ionic, triblock copolymer) [20]. The selection of the titanium precursor can impact the hydrolysis and condensation reactions that occur during the formation of the mesoporous network [21]. The type of surfactant used affects the shape of the titania nanoparticles [22], and calcination, which is typically performed to eliminate organic residues, influences the polymorph type of TiO_2 and the size of the crystalline grains [23]. As reported in the literature, the microemulsion synthesis method allows for a higher yield percentage of titania powder compared to other chemical processes. Specifically, the general trend is microemulsion > sol-gel > solvothermal > hydrothermal, with yields of 85%, 80%, 78%, and 75%, respectively [24]. In detail, the titania powder obtained through microemulsion synthesis can achieve high surface area (256 m^2 g^{-1}) with a small particle size (50 nm) [25]. The microemulsion process stands out as an environmentally friendly synthesis method in comparison to other approaches. It exhibits lower greenhouse emissions compared to biological routes and reduces the employ for organic solvents typically used in sol-gel and solvothermal processes [24]. The microemulsion process, commonly employed for producing titania nanoparticles, consists of a water-in-oil (W/O) system with a volume ratio of 1:2 separated by a surfactant/cosurfactant monolayer. However, the organic solvent still represents the large part of the microemulsion.

In this work, we propose a new synthesis protocol based on a microemulsion system with a W:O volume ratio of 1:1 and working at atmospheric pressure and low-temperature. The fine-tuning of the synthesis protocol was also conceived to improve the synthesis yield in view of an industrial-scale production.

II. MATERIALS AND METHODS

A. Chemicals

Tetraethyl orthotitanate (TEOT), Titanium butoxide (TiBUT), cyclohexane, 1-penthanol, cetylpyridinium bromide (CPB), methylene blue (MB), urea, and ultrapure water were purchased from Merck S.r.l. (Germany).

B. Synthesis

Titania nanoparticles were obtained by microemulsion synthesis with reflux method. The microemulsion consists of an oil phase, composed of 30.0 mL of cyclohexane (0.28 mol) and 1.5 mL 1-pentanol (13.80 mmol) droplet into the aqueous phase, composed of 30.0 mL water, 1.0 g CPB (2.60 mmol), and 0.6 g urea (10.00 mmol), mixed under vigorous stirring. After that, 2.5 g Titanium precursor was added to the microemulsion. The mixture was stirred at room temperature for 1 h, then transferred in a three-neck flask, and refluxed for 48 h at 70 °C. The powder was collected by centrifuge, washed in ethanol, and finally calcined at 450 or 600 °C for 4 h. In Table 1 the precursor adopted in the synthesis, the calcination temperature, and yield were reported.

Table 1. Summary of different specimens

Sample	Ti precuros	T calcination (°C)	Yield (%)
NT1	TEOT	600	80
NT2	TEOT	450	91
NT3	TiBUT	600	93
NT4	TiBUT	450	88

C. Characterization

Textural and morphological properties of titania nanoparticles were observed under the Scanning Electron Microscope (FE-SEM ZEISS SIGMA 300, Germany). The samples were observed at a high vacuum with an accelerating voltage of 10 kV. Crystallographic phase and crystallite size were determined using a SCINTAG diffractometer (San Francisco, USA) within the 2θ range of 2-70 ° at a rate of 3 min^{-1}. All the measurements were performed at room temperature using Cu Kα radiation (λ = 1.54 Å). The Scherrer equation calculated the crystallites size:

$$D = \frac{K\lambda}{(FWHM)cos\theta}$$

Where L is the crystallite size; K is a dimensionless shape factor with a value close to unity, 0.94 for spherical crystallites, λ is the X-Ray wavelength (1.5418 Å), Cosθ is the peak position 2θ/θ in radiant, and FWHM is the Full Width Half Maximum calculated by Origin.

Lambda 2 UV/Vis spectrometer (PerkinElmer, Canada) was used for the determination of the MB dye concentration. The UV/Vis spectrometer features double beam optics and recording the spectra over the 190–1100 nm range. A Beer–Lambert diagram was used to correlate the absorbance at 664 nm to MB concentration.

D. Photocatalytic activity

The degradation of MB was used to evaluate the photocatalytic activity of the synthesized materials under solar light irradiation. The photocatalyst [0.6 g L^{-1}] was added to a methylene blue solution [2.5 10^{-5} M]. The suspension was stirred in the dark for 30 min to reach the adsorption equilibrium before irradiation. Solar tests were performed in June at 35-38 °C, with an RH of 65% and South orientation. After irradiation, aliquots of 3.0 mL of the aqueous suspension were collected from the reactor and centrifuged at 6000 rpm for 15 min to remove the catalyst powder. The UV-Vis spectroscopy was used for the determination of the dye concentration. The following equation was used to calculate the photodegradation rate

of MB:

$$Degradation\ (\%) = \frac{(A_0 - A_t)}{A_0}$$

Where A_0 is the absorbance of initial MB, A_t is the absorbance of the solution after being irradiated for a period of t minutes. According to the first-order kinetics reaction, rate constant k (min^{-1}) was determined by using the following relation:

$$\ln\left(\frac{C_t}{C_0}\right) = -kt$$

C_t was the concentration after a period of t minutes, and C_0 represented the initial concentration. The degradation process was monitored following the absorbance at the maximum UV-Vis spectrum of the target molecule (664 nm). Since the degradation pathway for the selected dye is well known [26], the eventual formation of by-products was checked, monitoring the overall UV-Vis spectrum of the solutions recovered at different times.

III. RESULTS AND DISCUSSION

The SEM analysis was employed to evaluate the morphological structure of the nanoparticles. Figure 1 shows the SEM micrographs of the samples synthesized by reflux methods and P25 commercial titania nanoparticles. TiO_2 nanoparticles appear, for the most part, as agglomerates shapeless resulting from the aggregation of TiO_2 nanostructured grains characterized by an average size of around 30-50 nm, including the commercial titania P25. NT2 sample (Figure 1b), seems to be composed by titania nanograins organized in spheric nanoparticles of 900 nm size. These spherical particles appear as weakly sinterized. However, residual titania nanograins can be found on the surface of such aggregates. It is known that the calcination step, used for organic residues removal, usually improves the crystallinity degree but also affects the ordered mesoporous framework of TiO_2 that structurally collapses.

This effect is also evident in sample NT1 (Figure 1a), where the titania nanoparticles are strongly sintered. In samples NT2, NT3, and NT4 the grains of TiO_2 were weakly sintered, as shown in the SEM micrographs (Figure 1c,d). Moreover, NT3 (Figure 2c) seems to be the only sample where titania nanoparticles appear well distributed like in the commercial P25 sample (Figure 1e). The results suggest that the shape and structure of TiO_2 nanograins depend on the type of alkoxide used as a precursor together with the calcination temperature. At the same way, the reflux treatment method used for the polycondensation reaction do not influence shape, structure, and size of the synthesized nanoparticles.

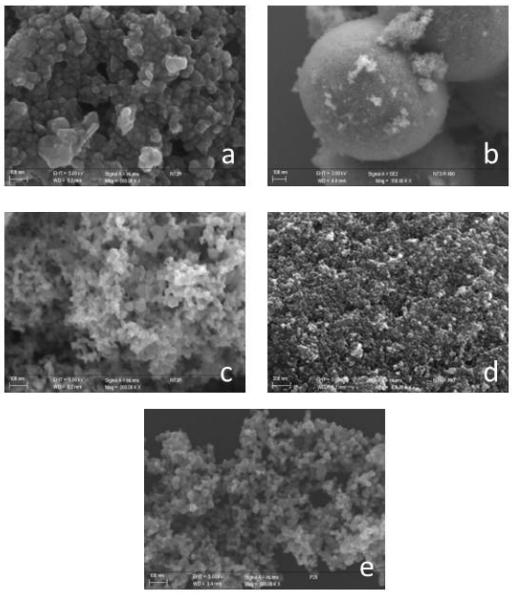

Figure 1. SEM micrographs of the samples (a) NT1, (b) NT2, (c) NT3, (d) NT4 and (e) P25.

Phase identification of the synthesized titania nanoparticles, and commercial P25 titania was performed by XRD analysis, and diffraction patterns are displayed in Figure 2. The diffraction peaks of the XRD patterns appear more narrow increasing the temperature from 450 to 600 °C. As shown in Figure 2, the formation of crystallites phase starts at 450 °C showing broad 2θ reflected peaks. When the calcination temperature was set at 600 °C, the peaks maintained the 2θ position and resulted narrower, suggesting a good crystallite formation obtaining a white powder. Anatase phase shows index reflection peaks at 25.3°; 37.7°; 48.2°; 53.95°; 55.0°, and 62.0°; meanwhile, rutile phase reflection peaks are 27.5˚; 36.1˚, 41.3˚; 62.8° and 68.8° (JCPDS No. 73-1764). Anatase and rutile phase are present in commercial P25 as well as NT1 with an average nano-crystallite size determined from peaks reflection of the anatase (101) and rutile (110) by the Scherrer formula are approximately 28-22 and 51-33 nm, respectively. In NT2, NT3, and NT4 the 2θ reflected peaks confirm the presence of anatase phase with an average size of anatase crystallites of about 8-10 nm. These results suggest that the titanium precursor may influence the crystallite phase formation. TEOT leads to the formation of anatase and rutile mixed phases, whereas TiBUT leads to the formation of the anatase phase.

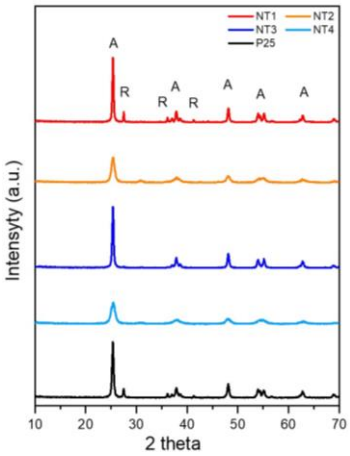

Figure 2. XRD spectra of the samples (a) NT1, (b) NT2, (c) NT3, (d) NT4 and (e) P25.

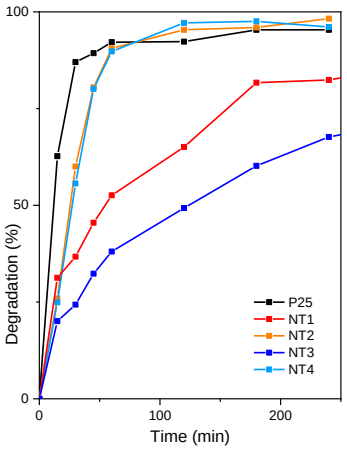

Figure 3. MB degradation under solar irradiation.

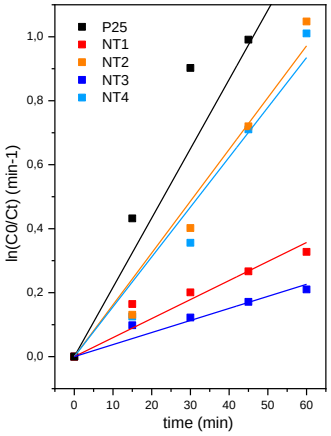

Figure 4. Kinetic linear simulation curves of MB degradation.

Spectroscopic and kinetic studies on the degradation of methylene blue (MB) were performed for NT1, NT2, NT3, and NT4 under solar irradiation and the photocatalytic activity was compared to the commercial P25 titania nanopowder. A solution of MB and synthetized titania nanoparticles were exposed under solar irradiation for 300 min. The initial concentration of MB was 2.5 x 10^{-5} M, and the catalyst dosage was 0.6 g L^{-1}. The UV-Vis spectra of the irradiated solution were recorded and monitored in the range 400–700 nm at different photoreaction times (after 15, 30, 60, 120, 180, 240 and 300 min). The degradation rate (D%) and the pseudo-first-order kinetics plot ($\ln(C_0/C_t)$) of MB adsorption versus time are shown in Figures 3-4.

The photocatalytic degradation of MB solutions operated by titania nanoparticles exposed to solar irradiation is reported in Figure 3. NT2, NT4, and P25 photocatalysts show a photodegradation rate of 90% after 60 minutes. On the other hand, the degradation rate of MB is around 52 % for NT1, and 40 % for sample NT3.

In Figure 4, the curve of $\ln(C_t/C_0)$ versus time is reported. The calculated kinetic parameters of MB degradation are shown in Table 2. The curves exhibit a good linear correlation, and the correlation coefficient (R^2) values are close to 1. Sample NT2, NT4, and P25 has the highest reaction rate constant of about 1.8 x 10^{-2} min^{-1} and an excellent photocatalytic activity. On the contrary, NT1 and NT3 show a low rate constant of about 2.77×10^{-3} and 1.73×10^{-3} respectively. The photocatalytic activity results higher than samples NT1 and NT3 and is improved by one order of magnitude from 2.77×10^{-3} min^{-1} to 1.79×10^{-2} min^{-1} and from 1.73×10^{-3} min^{-1} to 1.73×10^{-2} min^{-1}, changing the calcination temperature.

Table 2. Pseudo-first-order kinetic parameters of MB degradation under solar irradiation.

Sample	k (min^{-1})	R^2
P25	1.88×10^{-2}	0.96
NT1	2.77×10^{-3}	0.97
NT2	1.79×10^{-2}	0.98
NT3	1.73×10^{-3}	0.97
NT4	1.73×10^{-2}	0.98

As a result of the decreasing of the calcination temperature at 450 °C, the synthesized nanoparticles are less sinterized, showing the presence of anatase phase, and demonstrating an improved photocatalytic activity. In order to understand how the calcination temperature can influence the photocatalytic activity, further experiments are required to investigate the geometry of anatase TiO_2 single crystals and textural properties by using other techniques, such as N_2 physisorption, XPS, TEM, and UV-Vis-Abs analysis. As reported by Zhang [27], it is possible to increase the degradation rate of methyl orange solution to 93.63% after 60 min using a doped titania (Ag-TiO_2) characterized by the (001) crystal plane anatase with an

exposure ratio of 41.8 %. For the anatase phase TiO_2, the (001) plane corresponds to the high energy crystal surface, and the (101) plane is associated to the stable crystal surface. Therefore, the (001) crystal surface has a high energy and good reactivity. In photocatalytic reactions, photogenerated electrons transfer and accumulate on the (101) crystal planes of lower energy. On the other hand, photogenerated holes tend to accumulate on (001) crystal planes with high energy. This feature can effectively promote the separation of photogenerated electron-hole pairs, thereby improving their photocatalytic performance.

IV. CONCLUSION

Nanostructured TiO_2 was synthesized through an easy, low-temperature microemulsion route with a high synthesis yield. This study identifies the most efficient synthesis route for titania NPs production by using a W/O microemulsion in a volume ratio of 1:1, aimed to decrease the volume content of oil usually employed in the literature. The synthesis was conducted under atmospheric pressure (reflux method), obtaining a high synthetic yield (88-93%). All these parameters follow the green chemistry and sustainability approach. The samples were obtained as white powders with high crystallinity and purity. Samples were characterized from a structural, compositional, and morphological point of view. Among synthetized samples, NT2 shows an attractive shape and photoactivity behavior compared with the widely employed P25 commercial nanoparticles. The excellent photocatalytic performances were attributed to the crystal plane exposed and the morphological properties obtained by tuning the calcination temperature.

Acknowledgements: Authors gratefully acknowledge Sergio Lo Mastro for the technical support in SEM-EDS and XRD analysis at the Interdepartmental facility LIME Roma Tre University. The authors acknowledge financial support through the ERCOLE project (Le villE del paRCO di centocelLE) funded by Regione Lazio and Ministero dell'Istruzione e del Merito (MIUR) via research grants G12666, on BURL n. 99 21.\10.2021, of LAZIO INNOVA. Authors also thank DTC Lazio and PNRR CHANGES project. LT acknowledges Ministry of Education, Universities and Research: FINANZIAMENTO DIPARTIMENTI DI ECCELLENZA 2023-2027 (Art. 1, commi 314-337 Legge 11/12/2016, n. 232)

REFERENCES

[1] E. Sassoni, N. Roveri, G. W. Scherer, and E. Franzoni, "Durable self-cleaning coating for architectural surfaces by incorporation of TiO2 nano-particles into hydroxyapatite films," no. ii, 2018.

[2] D. Camuffo, M. Del Monte, and C. Sabbioni, "Origin and growth mechanisms of the sulfated crust on urban limestone," vol. 19, no. c, pp. 351–359, 1983.

[3] E. Franzoni, A. Fregni, R. Gabrielli, G. Graziani, and E. Sassoni, "Compatibility of photocatalytic TiO2-based finishing for renders in architectural restoration: A preliminary study," *Build Environ*, vol. 80, pp. 125–135, 2014, doi: 10.1016/j.buildenv.2014.05.027.

[4] K. Hashimoto, H. Irie, and A. Fujishima, "TiO 2 photocatalysis: A historical overview and future prospects," *Japanese Journal of Applied Physics, Part 1: Regular Papers and Short Notes and Review Papers*, vol. 44, no. 12, pp. 8269–8285, 2005, doi: 10.1143/JJAP.44.8269.

[5] T. Maggos, J. G. Bartzis, M. Liakou, and C. Gobin, "Photocatalytic degradation of NOx gases using TiO2-containing paint: A real scale study," *J Hazard Mater*, vol. 146, no. 3, pp. 668–673, 2007, doi: 10.1016/j.jhazmat.2007.04.079.

[6] A. M. Ramirez, K. Demeestere, N. De Belie, T. Mäntylä, and E. Levänen, "Titanium dioxide coated cementitious materials for air purifying purposes: Preparation, characterization and toluene removal potential," *Build Environ*, vol. 45, no. 4, pp. 832–838, 2010, doi: 10.1016/j.buildenv.2009.09.003.

[7] H. Babaizadeh and M. Hassan, "Life cycle assessment of nano-sized titanium dioxide coating on residential windows," *Constr Build Mater*, vol. 40, pp. 314–321, 2013, doi: 10.1016/j.conbuildmat.2012.09.083.

[8] N. T. Padmanabhan and H. John, "Titanium dioxide based self-cleaning smart surfaces: A short review," *J Environ Chem Eng*, vol. 8, no. 5, p. 104211, 2020, doi: 10.1016/j.jece.2020.104211.

[9] L. Ruggiero *et al.*, "Synthesis and Characterization of TEOS Coating Added With Innovative Antifouling Silica Nanocontainers and TiO2 Nanoparticles," *Front Mater*, vol. 7, no. June, 2020, doi: 10.3389/fmats.2020.00185.

[10] L. Tortora, G. Di Carlo, M. Moquera, G.Ingo, "Editorial: Nanoscience and Nanomaterials for the Knowledge and Conservation of Cultural Heritage" Frontiers in Materials, vol. 7, 2020, 10.3389/fmats.2020.606076.

[11] L. Pinho and M. J. Mosquera, "Titania-silica nanocomposite photocatalysts with application in stone self-cleaning," *Journal of Physical Chemistry C*, vol. 115, no. 46, pp. 22851–22862, 2011, doi: 10.1021/jp2074623.

[12] L. A. M. Carrascosa, R. Zarzuela, N. Badreldin, and M. J. Mosquera, "A Simple, Long-Lasting Treatment for Concrete by Combining Hydrophobic Performance with a Photoinduced Superhydrophilic Surface for Easy Removal of Oil Pollutants," *ACS Appl Mater Interfaces*, vol. 12,

no. 17, pp. 19974–19987, 2020, doi: 10.1021/acsami.0c03576.

[13] A. Olusegun *et al.*, “We are IntechOpen , the world ’ s leading publisher of Open Access books Built by scientists , for scientists TOP 1 %,” *Intech*, vol. i, no. tourism, p. 38, 2012, doi: 10.1016/j.colsurfa.2011.12.014.

[14] M. J. Gázquez, J. P. Bolívar, R. Garcia-Tenorio, and F. Vaca, “A Review of the Production Cycle of Titanium Dioxide Pigment,” *Materials Sciences and Applications*, vol. 05, no. 07, pp. 441–458, 2014, doi: 10.4236/msa.2014.57048.

[15] J. Jing, Y. Guo, S. Wang, F. Chen, L. Yang, and G. Qiu, “Recent Progress in Electric Furnace Titanium Slag Processing and Utilization: A Review,” *Crystals (Basel)*, vol. 12, no. 7, 2022, doi: 10.3390/cryst12070958.

[16] M. A. Irshad *et al.*, “Synthesis, characterization and advanced sustainable applications of titanium dioxide nanoparticles: A review,” *Ecotoxicol Environ Saf*, vol. 212, p. 111978, 2021, doi: 10.1016/j.ecoenv.2021.111978.

[17] P. Nyamukamba, O. Okoh, H. Mungondori, R. Taziwa, and S. Zinya, “Synthetic Methods for Titanium Dioxide Nanoparticles: A Review,” *Titanium Dioxide - Material for a Sustainable Environment*, 2018, doi: 10.5772/intechopen.75425.

[18] E. Grabowska, M. Marchelek, M. Paszkiewicz-Gawron, and A. Zaleska-Medynska, *Metal oxide photocatalysts*. Elsevier Inc., 2018. doi: 10.1016/B978-0-12-811634-0.00003-2.

[19] K. Lan *et al.*, “ Stable Ti 3+ Defects in Oriented Mesoporous Titania Frameworks for Efficient Photocatalysis ,” *Angewandte Chemie*, vol. 132, no. 40, pp. 17829–17836, 2020, doi: 10.1002/ange.202007859.

[20] E. M. Samsudin, S. B. A. Hamid, J. C. Juan, and W. J. Basirun, “Influence of triblock copolymer (pluronic F127) on enhancing the physico-chemical properties and photocatalytic response of mesoporous TiO 2,” *Appl Surf Sci*, vol. 355, pp. 959–968, 2015, doi: 10.1016/j.apsusc.2015.07.178.

[21] R. Zhang, A. A. Elzatahry, S. S. Al-Deyab, and D. Zhao, “Mesoporous titania: From synthesis to application,” *Nano Today*, vol. 7, no. 4, pp. 344–366, 2012, doi: 10.1016/j.nantod.2012.06.012.

[22] B. Bonelli, S. Esposito, and F. S. Freyria, “Mesoporous Titania: Synthesis, Properties and Comparison with Non-Porous Titania,” *Titanium Dioxide*, 2017, doi: 10.5772/intechopen.68884.

[23] A. M. Luís, M. C. Neves, M. H. Mendonça, and O. C. Monteiro, “Influence of calcination parameters on the TiO2 photocatalytic properties,” *Mater Chem Phys*, vol. 125, no. 1–2, pp. 20–25, 2011, doi: 10.1016/j.matchemphys.2010.08.019.

[24] F. Wu, Z. Zhou, and A. L. Hicks, “Life Cycle Impact of Titanium Dioxide Nanoparticle Synthesis through Physical, Chemical, and Biological Routes,” *Environ Sci Technol*, vol. 53, no. 8, pp. 4078–4087, 2019, doi: 10.1021/acs.est.8b06800.

[25] M. Andersson, L. Österlund, S. Ljungström, and A. Palmqvist, “Preparation of nanosize anatase and rutile TiO2 by hydrothermal treatment of microemulsions and their activity for photocatalytic wet oxidation of phenol,” *Journal of Physical Chemistry B*, vol. 106, no. 41, pp. 10674–10679, 2002, doi: 10.1021/jp025715y.

[26] A. Houas, H. Lachheb, M. Ksibi, E. Elaloui, C. Guillard, and J. M. Herrmann, “Photocatalytic degradation pathway of methylene blue in water,” *Appl Catal B*, vol. 31, no. 2, pp. 145–157, 2001, doi: 10.1016/S0926-3373(00)00276-9.

[27] L.-Y. Zhang *et al.*, “Preparation and Photocatalytic Property of Ag Modified Titanium Dioxide Exposed High Energy Crystal Plane (001),” vol. 10, no. 27, 2020.